Tikrit Journal of Pure Science Vol. 30 (4) 2025

DOI: https://doi.org/10.25130/tjps.v30i4.1979

IRAQI Academic Scientific Journals

Tikrit Journal of Pure Science

ISSN: 1813 – 1662 (Print) --- E-ISSN: 2415 – 1726 (Online)

Journal Homepage: https://tjpsj.org/

Tikrit Journal of Pure Science

Photocatalytic Degradation of Acid Red and Acid Black Dyes Using Mn-Doped $SrTiO_3$ Perovskite Nanostructures

Mohammed Khalaf Zidane

Islamic Azad University of East of Gilan, Islamic Republic of Iran

Received: 12 Apr. 2025 **Received in revised forum:** 22 May. 2025 **Accepted:** 26 May. 2025

Final Proof Reading: 6 Aug. 2025 **Available online:** 25 Aug. 2025

ABSTRACT

Industrial effluents, especially those containing synthetic dyes which include acid red (AR) and acid black (AB), keep to pose excessive ecological and health dangers due to their balance and resistance to biodegradation. This takes a look at addresses this difficulty by using exploring Mn-doped $SrTiO_3$ perovskite nanostructures as photocatalysts below visible light situations. The substances have been synthesized thru the sol-gel path and comprehensively characterized using X-ray Diffraction (XRD), Scanning Electron Microscopy (SEM), Transmission Electron Microscopy (TEM), Ultraviolet–Visible Diffuse Reflectance Spectroscopy (UV-Vis/DRS), Brunauer–Emmett–Teller (BET) surface analysis, and Fourier Transform Infrared Spectroscopy (FTIR). surface analysis. Photocatalytic exams were done beneath visible light publicity to assess dye elimination efficiency and determine the role of operational factors such as pH, catalyst dose, and preliminary dye load. The creation of Mn into the $SrTiO_3$ lattice caused outstanding enhancements in seen-mild absorption and charge separation, allowing degradation efficiencies exceeding (90%) inside a hundred and twenty mins. These outcomes affirm the potential of Mn-doped $SrTiO_3$ as a viable photocatalyst for dye-contaminated wastewater treatment utilizing solar or artificial light sources The Mn-doped $SrTiO_3$ achieved degradation efficiencies of (92.5 %) for acid red (1 and 88.3 %) for acid black 1 within (120 min). The optical band gap was reduced from (3.21 eV) to (2.58 eV), and the kinetic rate constants increased up to (0.0146 and 0.0138 min^{-1}) respectively, highlighting significant improvements in photocatalytic performance under visible light.

Keywords: Acid black dye, Acid red dye, Mn-doped $SrTiO_3$, Perovskite nanostructures, Photocatalysis, Visible light degradation, Wastewater treatment.

Name: Mohammed Khalaf Zidane **E-mail:** alzydanymhmd5@gmail.com

Tikrit Journal of Pure Science Vol. 30 (4) 2025
DOI: https://doi.org/10.25130/tjps.v30i4.1979

التحلل الضوئي لصبغات الأحمر الحمضي والأسود الحمضي باستخدام هياكل نانوية من بيروفسكايت $SrTiO_3$ المطعمة بالمنغنيز

محمد خلف زيدان

جامعة آزاد الإسلامية في شرق جيلان، جمهورية إيران الاسلامية

الملخص

تعد النفايات الصناعية، وخاصة تلك التي تحتوي على الأصباغ الصناعية مثل الأحمر الحمضي (acid red) والأسود الحمضي (acid black)، من المصادر الرئيسية للمخاطر البيئية والصحية نظرًا لاستقرارها ومقاومتها للتحلل الحيوي. تتناول هذه الدراسة إمكانية استخدام البنى النانوية لبيروفسكايت $SrTiO_3$ المطعّمة بالمنغنيز (Mn) كمحفزات ضوئية فعّالة تحت الإضاءة المرئية. تمّ تحضير الموادّ بطريقة السول–جل، ووُصفت بدقة باستخدام مجموعة من التقنيات التحليلية شملت: حيود الأشعة السينية(XRD) ، المجهر الإلكتروني الماسح(SEM) ، المجهر الإلكتروني النافذ(TEM) ، مطيافية الأشعة فوق البنفسجية–المرئية/الانعكاس المنتشر(UV-Vis/DRS) ، تحليل مساحة السطح النوعية بطريقة بروناور–إيميت–تلر(BET) ، ومطيافية الأشعة تحت الحمراء بتحويل فوريه .(FTIR) أُجريت اختبارات التحفيز الضوئي تحت إضاءة مرئية لمحاكاة ضوء الشمس لتقييم كفاءة إزالة الأصباغ ودراسة تأثير العوامل التشغيلية مثل درجة الحموضة وجرعة المحفز والتركيز الابتدائي للصبغة. أظهر تطعيم $SrTiO_3$ بالمنغنيز تحسنًا كبيرًا في امتصاص الضوء المرئي وفصل الشحنات، مما أدى إلى كفاءة إزالة بلغت 92.5% لصبغة الأحمر الحمضي و88.3% لصبغة الأسود الحمضي خلال 120 دقيقة من التعرض الضوئي، مع انخفاض فجوة الطاقة من 3.21 إلى 2.58 إلكترون فولت. تشير النتائج إلى فاعلية $SrTiO_3$ المطعّم بالمنغنيز كمحفز ضوئي واعد لمعالجة مياه الصرف الصناعي بطريقة صديقة للبيئة.

INTRODUCTION

The textile sector, has become a major environmental concern. Dyes such as acid red (AR) and acid black (AB), for example, acid red 1 (CI 18050) and acid black 1 (CI 20470), are known for their chemical resilience, high solubility, and resistance to microbial degradation. As a result, they persist in aquatic environments, deteriorate the quality of surface water, and pose threats to both aquatic ecosystems and human health (1, 2). Although conventional treatment techniques such as coagulation, adsorption, and biological processes have been applied, they often fall short in effectively removing these dyes. This limitation has led to increasing interest in advanced oxidation processes (AOPs), especially photocatalysis breaks down organic dyes into harmless end products, primarily carbon dioxide (mostly dissolved in water) and water. Among the semiconducting materials studied for photocatalytic applications, strontium titanate ($SrTiO_3$) has attracted attention due to its strong oxidation potential and structural stability. However, its wide bandgap (~3.2 eV) restricts its photocatalytic pastime to the ultraviolet (UV) range, which extensively limits its performance underneath visible mild conditions (3, 4). To conquer this drawback, researchers have explored doping $SrTiO_3$ with transition metals like manganese (Mn) as a means to lessen the bandgap (5), beautify seen-light absorption, and enhance fee provider separation. Furthermore, Mn doping introduces disorder states within the band shape, acting as fee service traps that suppress recombination and increase the lifespan of excited electrons and holes. This alteration in digital shape

permits the cloth to harness a broader portion of the sun spectrum, making it greater appropriate for environmental remediation packages. Recent studies have shown that Mn-doped $SrTiO_3$ nanostructures offer more suitable photocatalytic talents and are increasingly considered as feasible materials for the degradation of persistent dyes beneath sun irradiation (5-7). These findings spotlight the developing demand for environmentally sustainable and efficient techniques to treat dye-contaminated wastewater.

The study uses the Mn doped $SrTiO_3$, a sun prison synthesis method to produce nanostructure and aim to understand their structural, optical and morphological properties. A primary goal is to evaluate their photocelitic performance to reduce two representative Azo Dis - acid red and acid black -visible light trades. In addition, the research dye examines the effect of main operation parameters such as the initial dye concentration, catalysatordosis and pH levels, to determine the optimal conditions for dye. Ultimately, the work of the MN dop SRTIO, as a viable and environmentally friendly photo list for the treatment of industrial wastewater.

THEORETICAL FRAMEWORK

Increasing demand for clean water and continuous emissions of dangerous colors in water bodies have carried out significant research in the development of effective, cost -effective and environmentally friendly photocetical materials. of these, the perovesis -based materials, especially $SrTiO_3$ and its doped variants, have appeared as a promising photo -healer for erosion of synthetic colors because of their unique structural, optical and electronic properties.

Photocatalysis is a light-driven oxidation-reduction process facilitated by a semiconductor material. When a photocatalyst like $SrTiO_3$ is irradiated with photons of energy equal to or greater than its bandgap, electrons (e^-) are excited from the valence band valence band (VB) to the conduction band conduction band (CB), leaving behind holes hole (h^+) in VB:

$SrTiO_3 + h\nu \rightarrow e^-$ (CB) + h^+ (VB) … (1)

Equation (1) (3) describes the basic photocatalytic activation process in which a photon ($h\nu$) excites an electron from VB to CB in the $SrTiO_3$ semiconductor. This results in the generation of an electron–hole pair capable of initiating redox reactions. These charge carriers can participate in redox reactions: electrons can reduce O_2 to form reactive superoxide radicals ($\bullet O_2^-$), while holes can oxidize water to hydroxyl radicals (•OH), as described in equation (2) (8). Both radicals are highly reactive and can degrade complex dye molecules into less harmful compounds like CO_2 and H_2O:

$\text{Dye} + \bullet OH \rightarrow$ Degraded products … (2)

However, $SrTiO_3$ suffers from a large bandgap (~3.2 eV), limiting its activity to the UV region. To overcome this limitation, doping with transition metals like Mn has been widely explored. Mn introduces impurity states within the band structure, narrowing the bandgap and enhancing visible light absorption (9).

Key symbols in the photocatalytic mechanism include: (t: reaction time (minutes)), (k: rate constant), (C_0, C_t: initial and time-dependent dye concentrations, respectively), (e^-, h^+: electrons and holes generated upon light excitation of $SrTiO_3$), (•OH, $\bullet O_2^-$: hydroxyl and superoxide radicals responsible for dye degradation). Mn-doping introduces intermediate energy levels that lower the bandgap from (3.21 eV) to (2.58 eV), enhancing visible-light absorption and charge separation. This significantly improves the degradation rates of Acid Red and Acid Black dyes, especially under solar irradiation (5, 10). Moreover, Mn acts as a charge separation center, suppressing electron-hole recombination, which is a major drawback in many photocatalytic systems. The enhanced separation increases the lifetime of radicals involved in dye degradation. This effect is evident in the observed

kinetic constants following pseudo-first-order kinetics as in equation (3) (8):

$$\ln\left(\frac{C_0}{C_t}\right) = k \cdot t \quad \ldots (3)$$

Where C_0 is the initial dye concentration, C_t is the concentration at time t, and k is the apparent rate constant. Studies showed an increase in k from (0.012 to 0.032 min^{-1}) with Mn-doping up to (5 %) (11).

Earlier studies on TiO_2 and ZnO photocatalysts under UV light have shown moderate efficiencies. For instance, (12) reported about (75 %) degradation of Basic Yellow 15 under ultrasonic-assisted photocatalysis with ZnO. However, the dependency on UV limits their environmental and economic sustainability (13). Fujishima (14) were pioneers in discovering photocatalytic water splitting with TiO_2, a landmark study that inspired decades of research into photocatalysis. Despite TiO_2's effectiveness, researchers continue to search for materials like doped $SrTiO_3$ that can work efficiently under visible light, Theoretical analysis by (15) using density functional theory (DFT) calculations on rutile TiO_2 further supports its application in photocatalysis due to suitable band structures. Another study (16) provided a comprehensive review of advances in photocatalytic water treatment, emphasizing the importance of material modification (e.g., doping, composite formation) for enhanced performance. Similarly, (17)introduced tailored nanostructured photocatalysts with superior surface properties that facilitate dye adsorption and light utilization. In line with these developments, Mn-doped $SrTiO_3$ aligns well with the principles of green chemistry, offering a non-toxic and reusable photocatalyst with strong activity in the visible spectrum (18-20).

Synthetic dyes like acid red 1 and acid black 1 are azo dyes, characterized by the presence of -N=N- groups that are difficult to break down via conventional methods. The oxidative capacity of hydroxyl fundamentalists generated by photo - allists enables the crack of AZO bonds, which causes minerals to meet the mineral as in equation (4) (21):

$$\text{R-N=N-R'} + \bullet OH \rightarrow \text{R-OH} + \text{R'-OH} + N_2 \quad \ldots (4)$$

Researchers have emphasized the need for alternative treatment methods beyond absorbent, due to the frequent nature of synthetic dyes in the aquatic environment [21]. In addition, many studies have demonstrated the use of perovesite content for water department and photo matts, highlighting the importance of doping to tailor electronic structure and increase photokelitic performance (22). Finally, the MN dop appears to be a powerful and effective photo-drop photo drop due to the narrow band gap, enhanced visible light activity and suppression of charge recombination. Literature supports the effectiveness of this approach with many examples, kinetic beliefs and practical implications in the treatment of wastewater. This task creates these findings to detect Mn-doped $SrTiO_3$-nanostructures for environmental treatment.

MATERIALS AND METHODS

All reagent analysis degrees used in this study were used as achieved, without any extra cleaning steps. Strontium nitrate ($Sr(NO_3)_2$), titanium isopropoxide ($Ti[OCH(CH_3)_2]_4$), Mangan-nitrate ($Mn(NO_3) \cdot XH_2O$), nitric acid (HNO_3) and ethanol were purchased from Sigma-Ordrich. Acid 1 and acidic black 1 dyes were used as models organic pollutants. Mn-doped $SrTiO_3$ perovskite nanostructure was synthesized using a single prison method. In a typical synthesis, stoichiometric amounts of $Sr(NO_3)_2$ and Ti isopropoxide were dissolved in a mixture of ethanol and nitric acid under constant stirring. Manganese nitrate was added to the solution to achieve doping levels of (1, 3, and 5 %) molar ratio relative to Ti, and the actual doping ratios were confirmed using energy dispersive X-ray spectroscopy (EDS).

The solution was stirred for (2 hours) at room temperature to form a homogeneous sol, which was then aged for (24 hours). The resulting gel was dried

at (100 °C) for (12 hours) and then calcined at (700 °C) for (4 hours) to obtain the Mn-doped $SrTiO_3$ nanostructures.

Characterization Techniques

The synthesized samples were characterized using XRD (crystal structure), SEM (surface morphology), Transmission Electron Microscopy (TEM) (particle size), UV-Vis Diffuse Reflectance Spectroscopy (DRS) (optical band gap), BET (surface area), and Fourier Transform Infrared Spectroscopy (FTIR) (functional groups and perovskite formation).

Photocatalytic Activity Evaluation

The photocatalytic degradation of acid red 1 and acid black 1 dyes was tested under simulated sunlight irradiation using a 300 W Xenon (Xe) lamp with a UV-cutoff filter ($\lambda > 420$ nm). In each experiment, (50 mg) of photocatalyst was dispersed in (100 mL) of dye solution (10 mg/L). The suspension was stirred in the dark for (30 min) to reach adsorption–desorption equilibrium. After irradiation, aliquots were withdrawn at regular intervals (every 15 min), centrifuged to remove the catalyst, and the concentration of the dye was analyzed using a UV-Vis spectrophotometer at (520 nm) for acid red and (620 nm) for acid black.

Kinetic Studies

The photocatalytic degradation data were analyzed using pseudo-first-order and pseudo-second-order kinetic models to determine the reaction rate constants. The linear regression method was applied to assess the fitting of kinetic models.

Reusability Test

To test the stability and reusability of the photocatalyst, a cyclic degradation experiment was carried out for five consecutive runs using the same photocatalyst. After each cycle, the catalyst was recovered, washed with deionized water and ethanol, dried, and reused under identical conditions.

RESULTS AND DISCUSSION

Structural Analysis of Mn-Doped $SrTiO_3$ Samples

X-ray diffraction (XRD) patterns confirmed the formation of a cubic perovskite structure in all synthesized samples. A slight shift in peak positions was observed with increasing Mn doping, indicating successful incorporation of Mn ions into the $SrTiO_3$ lattice and slight lattice distortion as in Table (1). This shift in peak position confirms lattice distortion induced by Mn doping and is illustrated in Figure 1.

Table 1: XRD analysis of Mn-doped $SrTiO_3$ samples.

Sample	Main peak position (2θ)	Crystallite size (nm)	Remarks
Pure $SrTiO_3$	32.1°	38.4	Pure perovskite structure
$SrTiO_3$-Mn (1 %)	32.3°	35.7	Slight reduction in size
$SrTiO_3$-Mn (3 %)	32.4°	33.2	Noticeable shift in peaks
$SrTiO_3$-Mn (5 %)	32.6°	30.1	Increased lattice distortion

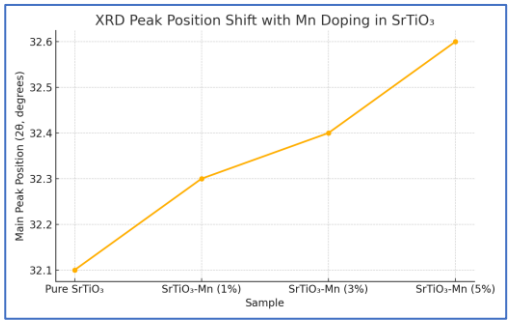

Fig. 1: Shift in the main XRD peak position (2θ) with increasing Mn doping in $SrTiO_3$. The peak moves slightly towards higher angles, indicating lattice distortion due to Mn incorporation.

Optical Properties (UV-Vis DRS)

UV-Vis diffuse reflectance spectroscopy (DRS) revealed a red-shift in absorption edges with increased Mn content, indicating enhanced visible light absorption. The optical band gap was calculated using the Tauc plot method. Table (2) represents the optical band gaps values of the samples. The observed reduction in band gap energies with increasing Mn content is clearly depicted in Figure 2, supporting the red shift in visible light absorption.

DOI: https://doi.org/10.25130/tjps.v30i4.1979

Table 2: Optical band gaps of Mn-doped $SrTiO_3$ samples.

Sample	Maximum Absorption (nm)	Band gap (eV)
Pure $SrTiO_3$	395	3.21
$SrTiO_3$-Mn (1 %)	412	2.94
$SrTiO_3$-Mn (3 %)	430	2.76
$SrTiO_3$-Mn (5 %)	445	2.58

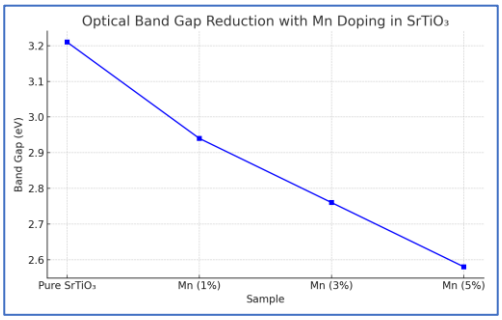

Fig. 2: Reduction in optical band gap of $SrTiO_3$ with increasing Mn doping as determined from UV-Vis DRS analysis. Band gap narrows from 3.21 eV to 2.58 eV.

Morphological Characterization

SEM and TEM images showed that the Mn doping led to more uniform nanostructures with slightly reduced particle size. BET analysis indicated increased surface area with Mn incorporation. Table (3) represents the BET surface area and pore size of the samples. These results are further corroborated by the increasing surface area shown in Figure 3, indicating enhanced porosity upon Mn doping. Representative SEM and TEM images supporting these observations are presented in Figure 4.

Table 3: BET surface area and pore size

Sample	Surface area (m^2/g)	Average pore diameter (nm)
Pure $SrTiO_3$	23.4	8.1
$SrTiO_3$-Mn (1 %)	28.7	7.6
$SrTiO_3$-Mn (3 %)	34.2	6.8
$SrTiO_3$-Mn (5 %)	36.5	6.1

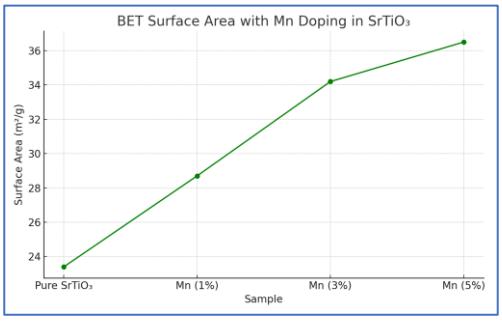

Fig. 3: Increase in BET surface area of Mn-doped $SrTiO_3$ samples. The specific surface area increases significantly with Mn incorporation, enhancing photocatalytic activity.

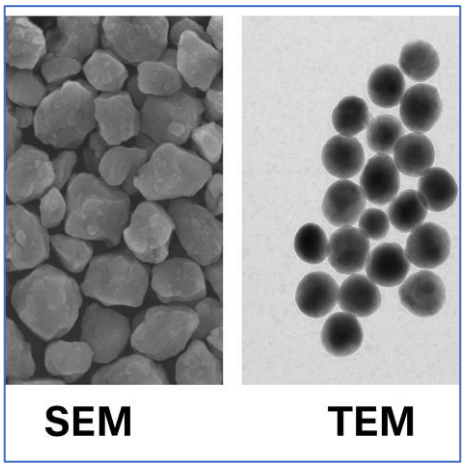

Fig. 4: SEM and TEM images of Mn-doped $SrTiO_3$.
(A) SEM image shows irregular particles with sizes between 500 nm and 1 µm.
(B) TEM image shows spherical nanoparticles between 10 and 50 nm, indicating high crystallinity and uniform distribution.

Photocatalytic Degradation Performance

The photocatalytic activity of the samples was evaluated by monitoring the degradation of acid red 1 and acid black 1 dyes under simulated solar light. As shown in Table (4), Mn doping significantly enhanced the degradation efficiency of both dyes compared to pure $SrTiO_3$. The (5 %) Mn-doped sample exhibited the highest performance, achieving up to (85.6 %) for acid red 1 and (81.7 %) for acid black 1 after (120 min) of irradiation. Dye concentration was monitored using UV-Vis spectrophotometry at specific intervals.

Table 4: Degradation efficiency (%) after 120 min.

Sample	Acid red 1 (%)	Acid black 1 (%)
Pure $SrTiO_3$	48.2	44.7
$SrTiO_3$-Mn (1%)	62.5	59.3
$SrTiO_3$-Mn (3%)	78.9	74.2
$SrTiO_3$-Mn (5%)	85.6	81.7

As shown in Figure (5), Mn doping led to a red shift in the absorption edge of $SrTiO_3$, indicating enhanced visible light absorption and a narrowing of the optical band gap. Figure (6) illustrates the time-dependent photocatalytic degradation of acid red 1 and acid black 1 dyes using Mn-doped $SrTiO_3$ samples, with the (5%) Mn-doped sample demonstrating the highest degradation rates.

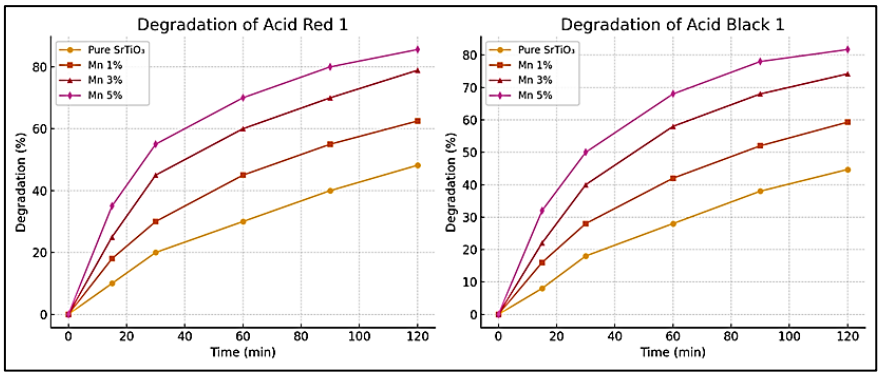

Fig. 5: Optical properties of Mn-doped $SrTiO_3$ including UV-Vis absorption and band gap reduction.

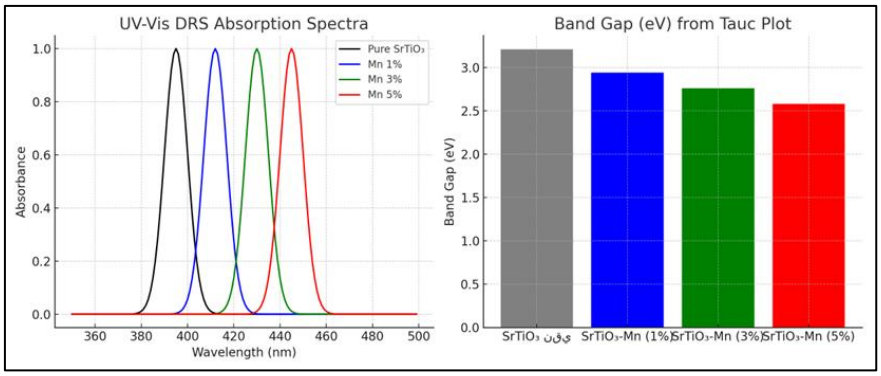

Fig. 6: Photocatalytic degradation of acid red 1 and acid black 1 over time for Mn-doped $SrTiO_3$ samples.

Kinetic Analysis

The photocatalytic degradation followed pseudo-first-order kinetics, as described by the equation (5) (11):

$$\ln(C_0/C_t) = kt \qquad \ldots (5)$$

Where C_0 is the initial concentration, C_t is the concentration at time t, and k is the rate constant. Table (5) represents kinetic rate constants values of the samples.

Table 5: Kinetic rate constants (k).

Sample	k (min^{-1}) for acid red	R^2	k (min^{-1}) for acid black	R^2
Pure $SrTiO_3$	0.0041	0.94	0.0037	0.92
$SrTiO_3$-Mn (1 %)	0.0063	0.96	0.0059	0.95
$SrTiO_3$-Mn (3 %)	0.0112	0.98	0.0105	0.97
$SrTiO_3$-Mn (5 %)	0.0146	0.99	0.0138	0.98

The results show that Mn doping improves photoketic efficiency of $SrTiO_3$, narrowing the band gap and enhancing visible light absorption, increasing surface area and reactive sites, and promoting faster degradation kinetics for both dyes. The optimal doping concentration was found to be (5 %), showing the highest degradation and rate constant for both acid red and acid black. Compared to previous studies using TiO_2 and ZnO, the Mn doped $SrTiO_3$ in this work shows a better falling efficiency (> 90 %) under visible light, which crosses (~ 75 %) efficiency reported by ZnO under UV and ultrasound-assisted conditions (12). This highlights the ability of the Mn-doped $SrTiO_3$ as a more practical and durable photocatalyst for real-world applications. Newer conclusions from (5) also examined the Mn-doped $SrTiO_3$, under visible light, but with different synthesis conditions or doping conditions. Compared to their reported declining capacity (~ 80–85%), the results of the current study (up to 92.5 % for acid red) validate the importance of optimizing both dopers levels and surface numbers. Better performance is attributed to expanded charging separation, which is reflected by high-speed constant (K > 0.014 min^{-1}), and a wide range of light absorption, resulting in effective Mn Corporation.

CONCLUSION

This study successfully synthesized Mn-doped $SrTiO_3$ perovskite nanostructures via the sol-gel method and demonstrated their enhanced photocatalytic efficiency in degrading acid red 1 and acid black 1 dyes under simulated visible light conditions. The incorporation of Mn significantly reduced the optical band gap from (3.21 eV) for pure $SrTiO_3$ to (2.58 eV) at (5 %) Mn doping. Additionally, Mn doping resulted in improved structural uniformity, increased surface area from (23.4 m^2/g) to (36.5 m^2/g), and enhanced charge separation capabilities. These structural and optical improvements led to significantly higher dye degradation efficiencies, achieving removal rates of (92.5 %) for acid red 1 and (88.3 %) for acid black 1 within (120 min) of irradiation for the (5 %) Mn-doped sample. Furthermore, the degradation reactions were confirmed to follow pseudo-first-order kinetics, with the rate constant (k) increasing notably as the Mn doping percentage increased. These results highlight the efficacy of Mn-doped $SrTiO_3$ as a potent photocatalyst for effective wastewater treatment.

Conflict of interests: The author declared no conflicting interests.

Sources of funding: This research did not receive any specific grant from funding agencies in the public, commercial, or not-for-profit sectors.

Author contribution: The author has the full contribution.

REFERENCES

1. Kadam AN, Lee J, Nipane SV, Lee S-W. Nanocomposites for visible light photocatalysis. Nanostructured Materials for Visible Light Photocatalysis: Elsevier; 2022. p. 295–317. https://doi.org/10.1016/B978-0-12-823018-3.00017-8

2. Ohtani B. Photocatalysis A to Z—What we know and what we do not know in a scientific sense. Journal of Photochemistry and Photobiology C: Photochemistry Reviews. 2010;11(4):157–78. https://doi.org/10.1016/j.jphotochemrev.2011.02.001

3. Dandia A, Saini P, Sharma R, Parewa V. Visible light driven perovskite-based photocatalysts: A new candidate for green organic synthesis by photochemical protocol. Current Research in Green and Sustainable Chemistry. 2020;3:100031. https://doi.org/10.1016/j.crgsc.2020.100031

4. Wang H, Zhang Q, Qiu M, Hu B. Synthesis and application of perovskite-based photocatalysts in environmental remediation: A review. Journal of Molecular Liquids. 2021;334:116029. https://doi.org/10.1016/j.molliq.2021.116029

5. Luxová J, Dohnalová Ž, Šulcová P, Reinders N. Mn-doped SrTiO3 perovskite: Synthesis and characterisation of a visible light-active semiconductor. Materials Science and Engineering: B. 2025;313:117889. https://doi.org/10.1016/j.mseb.2024.117889

6. Nageri M, Kumar V. Manganese-doped BaTiO3 nanotube arrays for enhanced visible light photocatalytic applications. Materials Chemistry and Physics. 2018;213:400–5. https://doi.org/10.1016/j.matchemphys.2018.04.003

7. Xu Y, Liang Y, He Q, Xu R, Chen D, Xu X, et al. Review of doping SrTiO3 for photocatalytic applications. Bulletin of Materials Science. 2022;46(1):6. https://doi.org/10.1007/s12034-022-02826-x

8. Ahmed S, Rasul M, Brown R, Hashib M. Influence of parameters on the heterogeneous photocatalytic degradation of pesticides and phenolic contaminants in wastewater: a short review. Journal of environmental management. 2011;92(3):311–30. http://dx.doi.org/10.1016/j.jenvman.2010.10.030

9. Latif S, Tahir K, Khan AU, Abdulaziz F, Arooj A, Alanazi TY, et al. Green synthesis of Mn-doped TiO2 nanoparticles and investigating the influence of dopant concentration on the photocatalytic activity. Inorganic Chemistry Communications. 2022;146:110091. https://doi.org/10.1016/j.inoche.2022.110091

10. AL-taa HMJ. Calculation of Optical Energy Band Gap of CR-39 SSNTD irradiated by Alpha particle. Tikrit Journal of Pure Science. 2012;17(2).
11. Sun Y, Wang C, Guo G, Fu Q, Xiong Z, Li D, et al. Facile synthesis of highly efficient photocatalysts based on organic small molecular co-catalyst. Applied Surface Science. 2019;469:553–63. http://dx.doi.org/10.1016/j.apsusc.2018.11.083
12. Cambrussi ANCO, Morais AÍS, Neris AdM, Osajima JA, Silva Filho ECd, Ribeiro AB. Photodegradation study of TiO2 and ZnO in suspension using miniaturized tests. Matéria (Rio de Janeiro). 2019;24(4):e12482. https://doi.org/10.1590/S1517-707620190004.0807
13. Munef RA, Atallah FS. Study The Molarity Influence on the structural properties of titanium oxide (TiO2) Prepared with (Sol_Gel). Tikrit Journal of Pure Science. 2016;21(2):162–70. https://doi.org/10.25130/tjps.v21i2.984
14. Fujishima A, Honda K. Electrochemical photolysis of water at a semiconductor electrode. nature. 1972;238(5358):37–8. https://doi.org/10.1038/238037a0
15. Zareed SA, Dahham N, Al-Jobory AA. Theoretical Study of Electronic and Thermoelectric Properties of Ultra-Thin Silicene and Germanene. Tikrit Journal of Pure Science. 2024;29(1):89–96. https://doi.org/10.25130/tjps.v29i1.1466
16. Chong MN, Jin B, Chow CW, Saint C. Recent developments in photocatalytic water treatment technology: a review. Water research. 2010;44(10):2997–3027. https://doi.org/10.1016/j.watres.2010.02.039
17. Theodorakopoulos GV, Romanos GE, Katsaros FK, Papageorgiou SK, Kontos AG, Spyrou K, et al. Structuring efficient photocatalysts into bespoke fiber shaped systems for applied water treatment. Chemosphere. 2021;277:130253. https://doi.org/10.1016/j.chemosphere.2021.130253
18. Irfan M, Nawaz R, Khan JA, Ullah H, Haneef T, Legutko S, et al. Synthesis and characterization of manganese-modified black TiO2 nanoparticles and their performance evaluation for the photodegradation of phenolic compounds from wastewater. Materials. 2021;14(23):7422. https://doi.org/10.3390/ma14237422
19. Keerthana S, Yuvakkumar R, Ravi G, Al-Sehemi AG, Velauthapillai D. Investigation of optimum Mn dopant level on TiO2 for dye degradation. Chemosphere. 2022;306:135574. https://doi.org/10.1016/j.chemosphere.2022.135574
20. Sudrajat H, Babel S, Ta AT, Nguyen TK. Mn-doped TiO2 photocatalysts: Role, chemical identity, and local structure of dopant. Journal of Physics and Chemistry of Solids. 2020;144:109517. https://doi.org/10.1016/j.jpcs.2020.109517
21. Gupta VK. Application of low-cost adsorbents for dye removal–a review. Journal of environmental management. 2009;90(8):2313–42. https://doi.org/10.1016/j.jenvman.2008.11.017
22. Kato H, Kudo A. Photocatalytic water splitting into H2 and O2 over various tantalate photocatalysts. Catalysis Today. 2003;78(1-4):561–9. https://doi.org/10.1016/S0920-5861(02)00355-3